UDC 621.3.013 https://doi.org/10.20998/2074-272X.2025.3.10

B.I. Kuznetsov, T.B. Nikitina, I.V. Bovdui, K.V. Chunikhin, V.V. Kolomiets, I.V. Nefodova

# Simplified method for analytically determining the external magnetostatic field of uncertain extended technical objects based on near-field measurements

***Introduction.*** *An important scientific and technical problem of magnetism of uncertain extended energy-saturated objects - such as naval vessels and submarines is implementation of strict requirements for magnetic silence based on mathematical modeling of magnetic field, adequate to its real measurements.* ***The purpose*** *of the work is to develop a simplified analytical method for determining the external magnetostatic field of extended technical objects with uncertain magnetic field sources based on near-field measurement data using spherical and spheroidal sources in a Cartesian coordinate system.* ***Methodology.*** *Forward problems of magnetostatics solved based on developed method of analytical calculation of magnetostatic field induction of spherical and spheroidal sources in Cartesian coordinate system based on near-field measurements. Geometric inverse problems of magnetostatics for solving prediction and control problems of magnetic silence of technical object calculated based on vector games solution. Both vector games payoff calculated as forward problems solutions Wolfram Mathematica software package used.* ***Results.*** *The results of prediction of magnetic field magnitude in far zone of extended technical objects based on designed multispheroidal magnetic field model in form of spatial elongated spheroidal harmonics in prolate spheroidal coordinate system and in form of multispherical magnetic field model in form of spatial spherical harmonics in spherical coordinate system using measurements near field and taking into account magnetic characteristics uncertainty of extracted technical objects.* ***Originality.*** *For the first time, a method of simplifying the mathematical modeling of the magnetic field of an uncertain long energy- saturated object developed based on development and application of method of analytical calculation of induction of magnetostatic fields of spherical and spheroidal sources in the Cartesian coordinate system. Unlike known methods developed method allows modeling magnetic field directly in Cartesian coordinate system based on near-field measurements without finding magnetic induction projection in prolate spheroidal coordinate system and in spherical coordinate system without their translation from prolate spheroidal coordinate system and in spherical coordinate system in Cartesian coordinate system and vice versa.* ***Practical value.*** *The possibility of a more than 10 times calculation time reduction of magnetic field induction of magnetic field elongated spheroidal sources and the possibility of a more than 4 times calculation time reduction of magnetic field induction of magnetic field spherical sources when magnetic field calculating of uncertain extended energy-saturated object based on development and application of analytical calculation method of magnetostatic field induction of spherical and spheroidal sources in the Cartesian coordinate system based on near-field measurements shown.* References 50, tables 2, figures 4.

*Key words:* **energy-saturated extended technical objects, magnetic field, multispheroidal model, magnetic silencing, extended spheroidal coordinate system, spatial extended spheroidal harmonics.**

***Проблема.*** *Важливою науково-технічною проблемою магнетизму невизначених протяжних енергонасичених об'єктів таких як військово-морські судна та підводні човни є реалізація жорстких вимог «магнітної тиші» на основі математичного моделювання магнітного поля, адекватного його реальним вимірюванням.* ***Метою*** *роботи є розробка спрощеного аналітичного методу визначення зовнішнього магнітостатичного поля протяжних технічних об'єктів з невизначеними джерелами магнітного поля на основі даних вимірів в ближній зоні з використанням сферичних та сфероїдальних джерел в декартовій системі координат.* ***Методологія.*** *Прямий метод проблеми магнітостатики вирішується на основі розробленого методу аналітичного розрахунку індукції магнітостатичного поля сферичних та сфероїдальних джерел в декартовій системі координат на основі вимірювань ближнього поля. Геометричні обернені задачі магнітостатики для вирішення проблем передбачення і контролю магнітної тиші технічного об'єкта обчислюються на основі розв'язання векторних ігор. Виграші обох векторних ігор обчислюються як рішення прямої проблеми з використанням програмного пакету Wolfram Mathematica.* ***Результати.*** *Результатом прогнозування є величини віддаленого магнітного поля протяжних технічних об'єктів на основі спроектованої мультисфероїдальної моделі магнітного поля в вигляді просторових витягнутих сфероїдальних гармонік в витягнутій сфероїдній системі координат, та в вигляді мультисферичної моделі магнітного поля в вигляді просторових сферичних гармонік у сферичній системі координат з використанням вимірювань ближнього поля з врахуванням невизначеності магнітних характеристик витягнутих технічних об'єктів.* ***Оригінальність.*** *Вперше розроблено метод спрощення математичного моделювання магнітного поля невизначеного протяжного енергонасиченого об'єкта на основі розробки та застосування методу аналітичного розрахунку індукції магнітостатичного поля сферичних та сфероїдальних джерел в декартовій системі координат. На відміну від відомих методів, розроблений метод дозволяє моделювати магнітне поле безпосередньо в декартовій системі координат на основі вимірювань ближнього поля без знаходження проекції магнітної індукції в витягнутій сфероїдальній системі координат та в сферичній системі координат без їх переводу із витягнутій сфероїдальній системі координат, та із сферичної системи координат, в декартову систему координат, чи навпаки.* ***Практична цінність.*** *Показана можливість скорочення, більше ніж у 10 разів, часу розрахунку індукції магнітного поля витягнутих сфероїдальних джерел магнітного поля, та можливість зменшення, більше ніж в 4 рази, часу розрахунку індукції магнітного поля сферичних джерел магнітного поля при обчисленні магнітного поля невизначеного протяжного енергонасиченого об'єкта на основі розробки та застосування методу аналітичного розрахунку індукції магнітостатичного поля сферичних і сфероїдальних джерел в декартовій системі координат на основі вимірювань ближнього поля.* Бібл. 50, табл. 2, рис. 4.

*Ключові слова:* **енергонасичені протяжні технічні об'єкти, магнітне поле, мультисфероїдальна модель, магнітна тиша, витягнута сфероїдна система координат, просторові протяжні сфероїдні гармоніки.**

**Introduction.** An important scientific and technical problem of modern magnetism of technical objects is implementation of strict requirements for external magnetic field level. This problem is especially acute for magnetism of spacecraft, naval vessel and submarines [1–4]. The success of solving the problem of magnetism of these technical objects is largely determined by the adequacy of mathematical models of the external magnetic field (MF) to the real values of the magnetic characteristics of these objects [5–7]. To measure the real characteristics of the MF of spacecraft, military ships and submarines, special magnetodynamic measuring stands have been developed, one of which is located at the Anatolii Pidhornyi Institute of Power Machines and Systems of the National Academy of Sciences of Ukraine [8]. Based on the experimentally measured values of the MF components on the bench, a mathematical model of the MF of technical object designed [9–11]. Then, based on the mathematical model of the technical object designed on the basis of measurements of the near MF, the values of the MF parameters in the far zone are calculated. This is the task of MF prediction [6]. Then, based on the calculated

values of the MF parameters in the far zone, the problem of calculating the parameters and coordinates of the location in the space of the technical object of the compensating sources of the MF is solved to meet the requirements for the parameters of the MF of the technical object [6, 7].

The most widely used sources of MF are point sources, the MF of which is described in a spherical coordinate system (SCS). The mathematical model of technical objects is often adopted in the form of a multiple dipole model (MDM). The parameters of the dipoles and the coordinates of their location in the space of the technical object are determined in the course of solving the geometric inverse problem of magnetostatics from the condition of minimizing the error between the measured and predicted by the model values of the parameters of the external MF at the specified points of measurement of space [6].

Despite the fact that the shape of military ships and submarines has a «cigar-shaped» appearance of elongated technical objects, mathematical models of the MF of such objects are also often adopted in MDM form. In the works of [12–16], the expediency of using mathematical models in the form of elongated ellipsoidal sources (EES) of MF, describing the parameters of the MF in prolate spheroidal coordinate systems (PSCS), is shown for such elongated technical objects.

On magnetodynamic stands, measurements of magnetic characteristics of technical objects are usually measured in Cartesian coordinate systems (CCS) related to the center of technical objects. In MDM of the MF of technical objects, the positions of dipole sources of the MF are also specified in CCS related to the center of technical objects. In addition, on magnetodynamic stands, magnetic characteristics of component units of electrical equipment of technical objects are often measured, which are also, as a rule, measured in CCS related to the center of these component units of electrical equipment of technical objects [17–19].

However, mathematical models of concentrated MF sources are calculated in SCS associated with the centers of these sources. Mathematical models of elongated MF sources are calculated in the form of prolate spheroidal MF sources in PSCS associated with the centers of these sources [20, 21].

In classical works on electrodynamics [22–31], solutions of the Laplace equation for the scalar potential of a MF in a SCS and in a PSCS are known. Accordingly, these solutions are written in terms of SCS and PSCS [20, 21]. But for practice, it is often necessary to work in terms of a CCS [32–34]. In addition, it is not the scalar potential that is practically important, but the projections of the magnetic induction.

In modern works, for example, related to the magnetic cleanliness of spacecraft [22–31] and magnetic silence of naval vessel and submarines [17–19], analytical formulas of magnetic induction projections in terms of SCS and PSCS are derived on the basis of solutions to the Laplace equation for the scalar potential of the MF outside the source. Furthermore, in the case of SCS, generalized formulas for the magnetic induction projections for the nth spherical harmonic are derived [35], whereas in the case of PSCS, this is not the case. Instead, only general formulas for the magnetic induction projections are presented, which require taking the derivatives of the scalar potential with respect to the PSCS coordinates [20, 21]. In some instances, for several first spherical harmonics (up to 4), for some reason, the associated Legendre polynomials are written out, thereby obtaining rather cumbersome formulas [21]. An additional inconvenience is the constant necessity to transform both the coordinates from CCS to SCS and the projections of magnetic induction from SCS to CCS (the situation is similar with PSCS). This presents a significant challenge when attempting to calculate the MF from multiple sources, particularly when these sources are both spherical and spheroidal.

The peculiarity of the considered energy-saturated elongated objects is the inaccurate knowledge of magnetic characteristics and their change in different operating modes. Such objects are called uncertain objects [5–7].

**The purpose of the work** is to develop a simplified analytical method for determining the external magnetostatic field of extended technical objects with uncertain magnetic field sources based on near-field measurement data using spherical and spheroidal sources in a Cartesian coordinate system.

**Definition of forward magnetostatics problem for spheroidal sources.** Consider analytical formulas for projections of magnetic induction in CCS for spheroidal harmonics of MF in PSCS. Consider multyspheroidal model of original MF of energy-saturated extended technical object in PSCS. Let us assume that initial MF of extended energy-saturated object generated using spheroidal MF sources located at technical object space points with coordinates ($x_i$, $y_i$, $z_i$) in CCS associated with the center of technical object (Fig. 1).

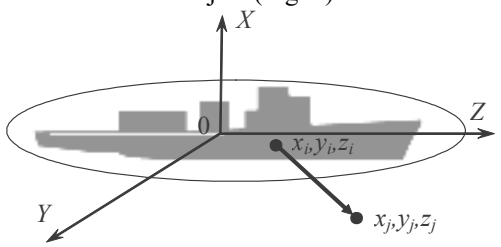


Fig. 1. Energy-saturated extended technical object

The relationship between the right triple of unit vectors $\{x, y, z\}$ of the CCS and the triple $\{\xi, \eta, \varphi\}$ of the PSCS has the form [12–14, 36]:

$$\begin{cases} x = c\sqrt{\left(\xi^2-1\right)\left(1-\eta^2\right)}\cos\varphi; \\ \qquad\qquad\qquad\qquad \xi \in [1,\infty]; \\ y = c\sqrt{\left(\xi^2-1\right)\left(1-\eta^2\right)}\sin\varphi; \Rightarrow \eta \in [-1,1]; \\ \qquad\qquad\qquad\qquad \varphi \in [0,2\pi], \\ z = c\xi\eta; \end{cases} \quad (1)$$

where $c$ is half the focal length of the spheroid whose foci lie on the $z$-axis at the points $\pm c$. From a geometric point of view, the triple $\{\xi, \eta, \varphi\}$ is a family of prolate spheroids ($\xi$=const), two-sheeted hyperboloids ($\eta$=const) and half-planes ($\varphi$=const) passing through the $z$-axis.

The surfaces of prolate spheroids $\xi$=const satisfy the equation [12–14, 36]

$$z^2\xi^{-2} + \left(x^2+y^2\right)\left(\xi^2-1\right)^{-1} = c^2, \quad (2)$$

for two-sheeted hyperboloids $\eta$=const satisfy the equation [12–14, 36]

$$z^2\eta^{-2} - \left(x^2+y^2\right)\left(1-\eta^2\right)^{-1} = c^2. \quad (3)$$

The solution of the Laplace equation in the PSCS with respect to the scalar potential of the MF for the external region $\xi>\xi_0$ outside the sources has the form [12–14]

$$U=\frac{1}{4\pi}\sum_{n=1}^{\infty}\sum_{m=0}^{n}Q_n^m(\xi)\left(c_n^m\cos m\varphi+s_n^m\sin m\varphi\right)P_n^m(\eta), \quad (4)$$

where $P_n^m$, $Q_n^m$ are the associated Legendre functions of the first and second kind, respectively, with degree $n$ and order $m$; $c_n^m$, $s_n^m$ are constant coefficients characterizing the MF in the PSCS.

The scalar potential $U(\xi, \eta, \varphi)$, presented in the PSCS (4), can also be considered in the CCS $U(x, y, z)$, expressing $\{\xi, \eta, \varphi\}$ through $\{x, y, z\}$ in (1). To do this, it is necessary to solve (2) and (3), respectively, with respect to $\xi$ and $\eta$. And to find $\varphi$, we divide the second equation by the first in (1). We obtain the following expressions:

$$\begin{cases}\xi=\dfrac{1}{2c}\left[\sqrt{x^2+y^2+(z+c)^2}+\sqrt{x^2+y^2+(z-c)^2}\right];\\ \eta=\dfrac{1}{2c}\left[\sqrt{x^2+y^2+(z+c)^2}-\sqrt{x^2+y^2+(z-c)^2}\right]; \quad (5)\\ \varphi=\arctan\dfrac{y}{x}.\end{cases}$$

We can find the projections of magnetic induction using the known relationship $\boldsymbol{B}=-\mu_0\mathrm{grad}U$. Moreover, it should be borne in mind that when taking partial derivatives with respect to $x$, $y$, $z$, the function $U(x, y, z)$ should be perceived as a complex $U[\xi(x, y, z), \eta(x, y, z), \varphi(x, y)]$ and act in accordance with the differentiation of a complex function.

Let us write the partial derivatives with respect to $x$, $y$, $z$ of the coordinates $\xi$, $\eta$, $\varphi$:

$$\begin{cases}\xi_x'=\dfrac{1}{2c}\left[\dfrac{x}{\sqrt{x^2+y^2+(z+c)^2}}+\dfrac{x}{\sqrt{x^2+y^2+(z-c)^2}}\right];\\ \xi_y'=\dfrac{1}{2c}\left[\dfrac{y}{\sqrt{x^2+y^2+(z+c)^2}}+\dfrac{y}{\sqrt{x^2+y^2+(z-c)^2}}\right]; \quad (6)\\ \xi_z'=\dfrac{1}{2c}\left[\dfrac{z+c}{\sqrt{x^2+y^2+(z+c)^2}}+\dfrac{z-c}{\sqrt{x^2+y^2+(z-c)^2}}\right];\end{cases}$$

$$\begin{cases}\eta_x'=\dfrac{1}{2c}\left[\dfrac{x}{\sqrt{x^2+y^2+(z+c)^2}}-\dfrac{x}{\sqrt{x^2+y^2+(z-c)^2}}\right];\\ \eta_y'=\dfrac{1}{2c}\left[\dfrac{y}{\sqrt{x^2+y^2+(z+c)^2}}-\dfrac{y}{\sqrt{x^2+y^2+(z-c)^2}}\right]; \quad (7)\\ \eta_z'=\dfrac{1}{2c}\left[\dfrac{z+c}{\sqrt{x^2+y^2+(z+c)^2}}-\dfrac{z-c}{\sqrt{x^2+y^2+(z-c)^2}}\right];\end{cases}$$

$$\begin{cases}\varphi_x'=-\dfrac{y}{x^2+y^2};\\ \varphi_y'=\dfrac{x}{x^2+y^2}.\end{cases} \quad (8)$$

Using recurrence relations for associated Legendre functions [36]:

$$(x^2-1)\frac{\mathrm{d}P_n^m(x)}{\mathrm{d}x}=-(n+1)xP_n^m(x)+(n-m+1)P_{n+1}^m(x), \quad (9)$$

$$(x^2-1)\frac{\mathrm{d}Q_n^m(x)}{\mathrm{d}x}=-(n+1)xQ_n^m(x)+(n-m+1)Q_{n+1}^m(x), \quad (10)$$

let's take the derivative with respect to t from the product of complex functions $P_n^m[x(t)]$ and $Q_n^m[y(t)]$:

$$\begin{aligned}&\frac{\mathrm{d}}{\mathrm{d}t}\left\{P_n^m[x(t)]Q_n^m[y(t)]\right\}=\\ &=\frac{1}{x^2-1}x_t'\left[-(n+1)xP_n^m(x)+(n-m+1)P_{n+1}^m(x)\right]Q_n^m(y)+ \quad (11)\\ &+\frac{1}{y^2-1}y_t'\left[-(n+1)yQ_n^m(y)+(n-m+1)Q_{n+1}^m(y)\right]P_n^m(x).\end{aligned}$$

Note that in (11) $x(t)$, $y(t)$ are simply abstract functions that have no relation to the coordinates (1). Now, using (5) – (8), (11) and the relation $\boldsymbol{B}=-\mu_0\mathrm{grad}U$, we write the $x$-projection of $\boldsymbol{B}$:

$$\begin{aligned}&B_x(x,y,z)=-\mu_0\frac{\partial}{\partial x}\left\{U\left[\xi(x,y,z),\eta(x,y,z),\varphi(x,y)\right]\right\}=\\ &=-\frac{\mu_0}{4\pi}\sum_{n=1}^{\infty}\sum_{m=0}^{n}\left\{\begin{aligned}&m\varphi_x'\left(s_n^m\cos m\varphi-c_n^m\sin m\varphi\right)Q_n^m(\xi)P_n^m(\eta)+\left(c_n^m\cos m\varphi+s_n^m\sin m\varphi\right)\times\\ &\times\left\{\frac{1}{\eta^2-1}\eta_x'\left[-(n+1)\eta P_n^m(\eta)+(n-m+1)P_{n+1}^m(\eta)\right]Q_n^m(\xi)+\right.\\ &\left.+\frac{1}{\xi^2-1}\xi_x'\left[-(n+1)\xi Q_n^m(\xi)+(n-m+1)Q_{n+1}^m(\xi)\right]P_n^m(\eta)\right\}\end{aligned}\right\}. \quad (12)\end{aligned}$$

After simplification and grouping relative to functions $Q_n^m(\xi)$ and $P_n^m(\eta)$ to reduce calculation time, we obtain the final formula for $B_x$:

$$B_x(x,y,z)=-\frac{\mu_0}{4\pi}\sum_{n=1}^{\infty}\sum_{m=0}^{n}\left\{\begin{array}{l}\left[m\varphi_x'\left(s_n^m\cos m\varphi-c_n^m\sin m\varphi\right)-(n+1)\left(\frac{\eta_x'\eta}{\eta^2-1}+\frac{\xi_x'\xi}{\xi^2-1}\right)\left(c_n^m\cos m\varphi+s_n^m\sin m\varphi\right)\right]\times\\ \times P_n^m(\eta)Q_n^m(\xi)+(n-m+1)\left[\frac{\eta_x'}{\eta^2-1}P_{n+1}^m(\eta)Q_n^m(\xi)+\frac{\xi_x'}{\xi^2-1}P_n^m(\eta)Q_{n+1}^m(\xi)\right]\times\\ \times\left(c_n^m\cos m\varphi+s_n^m\sin m\varphi\right)\end{array}\right\}. \quad (13)$$

Similarly, we obtain formulas for $B_y$, $B_z$ (note that in the case of $B_z$ the first term in the curly brackets is zero, since $\varphi_z' = 0$):

$$B_y(x,y,z)=-\frac{\mu_0}{4\pi}\sum_{n=1}^{\infty}\sum_{m=0}^{n}\left\{\begin{array}{l}\left[m\varphi_y'\left(s_n^m\cos m\varphi-c_n^m\sin m\varphi\right)-(n+1)\left(\frac{\eta_y'\eta}{\eta^2-1}+\frac{\xi_y'\xi}{\xi^2-1}\right)\left(c_n^m\cos m\varphi+s_n^m\sin m\varphi\right)\right]\times\\ \times P_n^m(\eta)Q_n^m(\xi)+(n-m+1)\left[\frac{\eta_y'}{\eta^2-1}P_{n+1}^m(\eta)Q_n^m(\xi)+\frac{\xi_y'}{\xi^2-1}P_n^m(\eta)Q_{n+1}^m(\xi)\right]\times\\ \times\left(c_n^m\cos m\varphi+s_n^m\sin m\varphi\right)\end{array}\right\}; \quad (14)$$

$$B_z(x,y,z)=-\frac{\mu_0}{4\pi}\sum_{n=1}^{\infty}\sum_{m=0}^{n}\left\{\begin{array}{l}\left[-(n+1)\left(\frac{\eta_z'\eta}{\eta^2-1}+\frac{\xi_z'\xi}{\xi^2-1}\right)\left(c_n^m\cos m\varphi+s_n^m\sin m\varphi\right)\right]P_n^m(\eta)Q_n^m(\xi)+\\ +(n-m+1)\left[\frac{\eta_z'}{\eta^2-1}P_{n+1}^m(\eta)Q_n^m(\xi)+\frac{\xi_z'}{\xi^2-1}P_n^m(\eta)Q_{n+1}^m(\xi)\right]\times\\ \times\left(c_n^m\cos m\varphi+s_n^m\sin m\varphi\right)\end{array}\right\}. \quad (15)$$

Note, that all the formulas (1) – (15) given above are for the case when the technical object is extended along the $z$ axis However, a more familiar coordinate system is also often considered, when the technical object is extended along the $x$ axis. If the technical object is extended along the $x$-axis, then the CCS must be rotated relative to the PSCS so that the $x$-axis takes the place of the $z$-axis, $y$ takes the place of $x$, and $z$ takes the place of $y$. In this case, the following replacement must be made in formulas (5) – (8): $x \to y$; $y \to z$; $z \to x$. And in the right-hand parts of formulas (13) – (15): $B_x \to B_y$; $B_y \to B_z$; $B_z \to B_x$.

**Definition of forward magnetostatics problem for spherical sources.** Let us consider analytical formulas for projections of magnetic induction in CCS using spherical harmonics. The relationship between the right triple of unit vectors $\{x, y, z\}$ in CCS and triple $\{r, \theta, \varphi\}$ in SCS has form [14, 36]:

$$\left\{\begin{array}{l}x=r\sin\theta\cos\varphi;\\ \qquad\qquad r\in[0,\infty];\\ y=r\sin\theta\sin\varphi;\Rightarrow\theta\in[0,\pi];\\ \qquad\qquad \varphi\in[0,2\pi];\\ z=r\cos\theta.\end{array}\right. \quad (16)$$

The solution of the Laplace equation in the SCS with respect to the scalar potential of the MF for the region outside the sphere $r>R_0$, where the sources of this field are contained, has the form [14]

$$U=\frac{1}{4\pi}\sum_{n=1}^{\infty}\frac{1}{r^{n+1}}\sum_{m=0}^{n}\left(g_n^m\cos m\varphi+h_n^m\sin m\varphi\right)\times\ldots \quad (17)$$
$$\ldots\times P_n^m(\cos\theta),$$

where $g_n^m$, $h_n^m$, are constant coefficients characterizing the MF in the SCS.

Using (16), we write the relationship between $\{x, y, z\}$ and $\{r, \cos\theta, \varphi\}$ this way:

$$\left\{\begin{array}{l}r=\sqrt{x^2+y^2+z^2};\\ \cos\theta=\dfrac{z}{\sqrt{x^2+y^2+z^2}};\\ \varphi=\arctan\dfrac{y}{x}.\end{array}\right. \quad (18)$$

Let us write the partial derivatives with respect to $x$, $y$, $z$ of the coordinate $r$ and the function $\cos\theta$ ($\varphi_x'$ and $\varphi_y'$ are already obtained by (8)):

$$\left\{\begin{array}{l}r_x'=\dfrac{x}{\sqrt{x^2+y^2+z^2}};\\ r_y'=\dfrac{y}{\sqrt{x^2+y^2+z^2}};\\ r_z'=\dfrac{z}{\sqrt{x^2+y^2+z^2}};\end{array}\right. \quad (19)$$

$$\begin{cases} (\cos\theta)'_x = -\dfrac{xz}{\sqrt{\left(x^2+y^2+z^2\right)^3}}; \\ (\cos\theta)'_y = -\dfrac{yz}{\sqrt{\left(x^2+y^2+z^2\right)^3}}; \\ (\cos\theta)'_z = \dfrac{x^2+y^2}{\sqrt{\left(x^2+y^2+z^2\right)^3}}. \end{cases} \quad (20)$$

Using the recurrence relation (9), we take the derivative with respect to $t$ of the product of complex functions $\dfrac{1}{r^{n+1}(t)}$ and $P_n^m[x(t)]$:

$$\frac{\mathrm{d}}{\mathrm{d}t}\left\{\frac{1}{r^{n+1}(t)}P_n^m[x(t)]\right\} = -r_t'\frac{n+1}{r^{n+2}}P_n^m(x) + \\ + \frac{1}{x^2-1}x_t'\left[-(n+1)xP_n^m(x)+(n-m+1)P_{n+1}^m(x)\right]\frac{1}{r^{n+1}}. \quad (21)$$

Proceeding in a similar manner as for spheroidal coordinates, using (8), (18) – (21) and the relation $\boldsymbol{B} = -\mu_0 \mathrm{grad} U$, we write the $x$-projection of $\boldsymbol{B}$:

$$B_x(x,y,z) = -\mu_0\frac{\partial}{\partial x}\{U[r(x,y,z),\cos\theta(x,y,z),\varphi(x,y)]\} = \\ = -\frac{\mu_0}{4\pi}\sum_{n=1}^{\infty}\sum_{m=0}^{n}\left\{\begin{array}{l} m\varphi_x'\dfrac{1}{r^{n+1}}\left(h_n^m\cos m\varphi - g_n^m\sin m\varphi\right)P_n^m(\cos\theta)+\left(g_n^m\cos m\varphi + h_n^m\sin m\varphi\right)\times \\ \times\left\{\begin{array}{l} -r_x'\dfrac{n+1}{r^{n+2}}P_n^m(\cos\theta)+\dfrac{1}{\cos^2\theta-1}(\cos\theta)'_x\times \\ \times\left[-(n+1)\cos\theta\cdot P_n^m(\cos\theta)+(n-m+1)P_{n+1}^m(\cos\theta)\right]\dfrac{1}{r^{n+1}} \end{array}\right. \end{array}\right\}. \quad (22)$$

After simplifying and grouping relative functions $P_n^m\cos\theta$ to reduce calculation time, we obtain the final formula for $B_x$:

$$B_x(x,y,z) = -\frac{\mu_0}{4\pi}\sum_{n=1}^{\infty}\frac{1}{r^{n+2}}\times \\ \times\sum_{m=0}^{n}\left\{\begin{array}{l} \left[m\varphi_x' r\left(h_n^m\cos m\varphi - g_n^m\sin m\varphi\right)-(n+1)\left(r_x'+\dfrac{(\cos\theta)'_x r\cos\theta}{\cos^2\theta-1}\right)\left(g_n^m\cos m\varphi + h_n^m\sin m\varphi\right)\right]\times \\ \times P_n^m(\cos\theta)+(n-m+1)\dfrac{(\cos\theta)'_x r}{\cos^2\theta-1}\left(g_n^m\cos m\varphi + h_n^m\sin m\varphi\right)P_{n+1}^m(\cos\theta) \end{array}\right\}. \quad (23)$$

Similarly, we obtain formulas for $B_y$, $B_z$ (note that in the case of $B_z$ the first term in the curly brackets is zero, since ($\varphi_z' = 0$):

$$B_y(x,y,z) = -\frac{\mu_0}{4\pi}\sum_{n=1}^{\infty}\frac{1}{r^{n+2}}\times \\ \times\sum_{m=0}^{n}\left\{\begin{array}{l} \left[m\varphi_y' r\left(h_n^m\cos m\varphi - g_n^m\sin m\varphi\right)-(n+1)\left(r_y'+\dfrac{(\cos\theta)'_y r\cos\theta}{\cos^2\theta-1}\right)\left(g_n^m\cos m\varphi + h_n^m\sin m\varphi\right)\right]\times \\ \times P_n^m(\cos\theta)+(n-m+1)\dfrac{(\cos\theta)'_y r}{\cos^2\theta-1}\left(g_n^m\cos m\varphi + h_n^m\sin m\varphi\right)P_{n+1}^m(\cos\theta) \end{array}\right\}. \quad (24)$$

$$B_z(x,y,z) = -\frac{\mu_0}{4\pi}\sum_{n=1}^{\infty}\frac{1}{r^{n+2}}\sum_{m=0}^{n}\left\{\begin{array}{l} \left[-(n+1)\left(r_z'+\dfrac{(\cos\theta)'_z r\cos\theta}{\cos^2\theta-1}\right)\left(g_n^m\cos m\varphi + h_n^m\sin m\varphi\right)\right]\times P_n^m(\cos\theta)+ \\ +(n-m+1)\dfrac{(\cos\theta)'_z r}{\cos^2\theta-1}\left(g_n^m\cos m\varphi + h_n^m\sin m\varphi\right)P_{n+1}^m(\cos\theta) \end{array}\right\}. \quad (25)$$

It is quite simple to calculate the MF created by several, for example $N_1$, spheroidal sources with coordinates $x_i$, $y_i$, $z_i$ relative to the center of the technical object $\{x_0, y_0, z_0\}=\{0, 0, 0\}$ and several, for example $N_2$, spherical sources that compensate for the MF in a given area, with coordinates $x_j$, $y_j$, $z_j$ relative to the center of the technical object. For this, we use the superposition principle and obtain, for example, for the projection:

$$B_x^{result}(x_p,y_p,z_p) = \\ = \sum_{i=1}^{N_1}B_{xi}(x_p-x_i,y_p-y_i,z_p-z_i)+ \\ + \sum_{j=1}^{N_2}B_{xj}(x_p-x_j,y_p-y_j,z_p-z_j),$$

where $B_{xi}$ is calculated by (13) with its parameters $c_i$, $c_{ni}^m$, $s_{ni}^m$ and $B_{xj}$ calculated by (23) with its parameters $g_{nj}^m$, $h_{nj}^m$. The same is true for other projections.

Thus, using formulas (13) – (15), (23) – (25), taking into account auxiliary formulas (5) – (8), (18) – (20), based on superposition principle, it is possible to calculate the MF at an arbitrary point in the region outside the spherical and spheroidal sources.

The advantage of these formulas over the known ones [12–14] are:

1) the projections of the magnetic induction in the CCS are explicitly written due to taking direct derivatives with respect to the CCS coordinates;

2) their generalization to the case of the *n*-harmonic;

3) there is no need to transform from one coordinate system to another, which is especially important in the case of calculating the MF from several spherical and spheroidal sources;

4) the relative compactness of the formulas.

**Definition of prediction geometric inverse magnetostatics problems.** Prediction problem implies design of mathematical model of MF of technical object based on experimentally measured values of MF components, as a rule, in near zone of technical object. The vast majority of mathematical models of MF of various technical objects – spacecraft, naval vessels and submarines – are MDMs.

The main advantage of MDMs is the ease of calculating components of MF generated by each magnetic dipole as a source of MF in rectangular coordinate system connected to center of technical facility. The main disadvantage of MDMs is large number of dipoles required to adequately simulate MF of technical object to actually measured values of MF on magnetodynamic stand. This is especially typical for modeling MF of elongated energy-saturated technical objects.

A significant simplification of modeling MF of elongated energy-saturated technical objects achieved by using elongated spheroidal MF sources in prolate spheroidal coordinate system. Moreover, to obtain required adequacy of mathematical model to actually measured characteristics of MF number of elongated spheroidal MF sources may be required tens or even hundreds of times less compared to number of dipole MF sources [37–42].

The obtained formulas (13) – (15) and (23) – (25) allow us to solve forward problem of magnetostatics. Using these formulas calculated components of MF induction in CCS at any point in space generated by spheroidal and spherical sources of MF. Naturally, in this case, coordinates of spatial location of these MF sources and their harmonics are specified.

The convenience of using these formulas lies in fact that components of projections of resulting MF in CCS are equal to sums of corresponding projections of MF induction of same in CCS, generated by all MF spheroidal and spherical sources.

Consider formulation of geometric inverse problem of design mathematical model of MF based on results of experimental measurements of MF. Introduce vector $\boldsymbol{G}$ of uncertainties in magnetic characteristics of technical object, due to inaccurate knowledge of initial values of magnetic characteristics of blocks of technical object, as well as changes in these magnetic characteristics in different operating modes [43–48].

Typically, MF measurements are carried out in CCS associated with the center of technical object. Let us introduce vector $\boldsymbol{Y}_M(\boldsymbol{G})$ of measured MF components.

Consider design of mathematical model of elongated energy-saturated object in form of set of spheroidal MF sources. Let us introduce vector $\boldsymbol{X}_P$ of desired parameters components of which are coordinates of spatial location and spatial harmonics of MF of these spheroidal MF sources. Then, vector $\boldsymbol{Y}_C(\boldsymbol{X}_P, \boldsymbol{G})$ calculated values of MF calculated based on (13) – (15).

Then solution of predictions geometric inverse problem of magnetostatics reduced to solution of vector game [49]

$$\boldsymbol{E}(\boldsymbol{X}_P, \boldsymbol{G}) = \boldsymbol{Y}_M(\boldsymbol{G}) - \boldsymbol{Y}_C(\boldsymbol{X}_P, \boldsymbol{G}). \qquad (26)$$

To calculate payoff vector game (26) it is necessary to repeatedly solved forward problem of magnetostatics (13) – (15) for elongated spheroidal MF sources.

**Definition of control geometric inverse magnetostatics problems.** The problem of controlling the magnetic silence of technical object is design of spatial arrangement and spatial harmonic sources of compensating MF. With the help of these compensating MF sources resulting MF of elongated energy-saturated technical object generated in such a way that stringent requirements for magnetic silence of energy-saturated technical object satisfied.

Note that the requirements for magnetic silence of technical object are usually imposed in the far zone. In particular, for military ships and submarines, requirements are imposed on magnitude and rate of change of MF components at control depth when an object moves at given speed.

The designed predictive mathematical model of MF of elongated energy-saturated object calculated based on experimental measurements of MF in near zone. Based on this prediction model of MF in near zone values of characteristics of MF of technical object calculated in far zone, which limited to meet requirements of magnetic silence of technical object.

Introduced uncertainty vector $\boldsymbol{G}_C$ of magnetic characteristics of energy-saturated technical object [43–48]. Then, based on the designed predictive model vector $\boldsymbol{B}(\boldsymbol{G})$ of initial values of magnetic characteristics of technical object, which determines its magnetic silence calculated.

To compensate for the original MF of technical object introduced dipole sources of compensating MF. Introduced vector $\boldsymbol{X}_C$ of required parameters for solving control geometric inverse problem of magnetostatics components of which are coordinates of spatial location and spatial harmonics of compensating dipoles.

Then vector $\boldsymbol{B}_C(\boldsymbol{X}_C, \boldsymbol{G})$ of calculated characteristics of magnetic silence of technical object calculated based on solution of forward problem of magnetostatics (23) – (25) for spherical MF sources.

Then solution of control geometric inverse problem of magnetostatics reduced to solution of vector game

$$\boldsymbol{B}_R(\boldsymbol{X}_C, \boldsymbol{G}_C) = \boldsymbol{B}(\boldsymbol{G}_C) + \boldsymbol{B}_C(\boldsymbol{X}_C). \qquad (27)$$

To calculate payoff vector game (27) it is necessary to repeatedly solved forward problem of magnetostatics (23) – (25) for spherical MF sources.

**Inverse magnetostatics problems solution method.** Solutions of both vector games (26) and (27) calculated by particle multi-swarm nonlinear optimization algorithms. Number of swarms calculated by number of components in vectors games (26), (27), so that with help of each swarm solution of scalar game calculated.

Each swarm $j$ contained two types of particles $i$. Position $x_{ij}(t)$ and movement velocity $v_{ij}(t)$ for first type particles calculated from conditions of minimizing payoff game along vectors $\boldsymbol{X}_P$ and $\boldsymbol{X}_C$ of desired parameters and described by following expressions:

$$\begin{aligned} v_{ij}(t+1) &= w_{1j}v_{ij}(t) + c_{1j}r_{1j}(t)\times\ldots \\ \ldots &\times H\left(p_{1ij}(t) - \varepsilon_{1ij}(t)\right)\left[y_{ij}(t) - \ldots\right. \\ \ldots &\left. - x_{ij}(t)\right] + c_{2j}r_{2j}(t)H\left(p_{2ij}(t) - \ldots\right. \\ \ldots &\left. - \varepsilon_{2ij}(t)\right)\left[y_j^*(t) - x_{ij}(t)\right]; \end{aligned} \tag{28}$$

$$x_{ij}(t+1) = x_{ij}(t) + v_{ij}(t+1). \tag{29}$$

Moreover, the best local $y_{ij}(t)$ and global $y_j^*(t)$ position of particle determined from condition of minimizing game vector along vectors $\boldsymbol{X}_P$ and $\boldsymbol{X}_C$ of desired parameters for games (26) and (27) respectively.

Position $g_{ij}(t)$ and movement velocity $u_{ij}(t)$, $z_{ij}(t)$ for second type particles calculated from conditions of minimizing payoff game along vectors $\boldsymbol{G}$ and $\boldsymbol{G}_C$ of magnetic characteristics uncertainty and described by following expressions:

$$\begin{aligned} u_{ij}(t+1) &= w_{2j}u_{ij}(t) + c_{3j}r_{3j}(t)H\times\ldots \\ \ldots &\times\left(p_{3ij}(t) - \varepsilon_{3ij}(t)\right)\left[z_{ij}(t) - \delta_{ij}(t)\right] + \ldots \\ \ldots &+ c_{4j}r_{4j}(t)H\left(p_{4ij}(t) - \varepsilon_{4ij}(t)\right)\times\ldots \\ \ldots &\times\left[z_j^*(t) - \delta_{ij}(t)\right]; \end{aligned} \tag{30}$$

$$g_{ij}(t+1) = \delta_{ij}(t) + u_{ij}(t+1). \tag{31}$$

Moreover, the best local $z_{ij}(t)$ and global $z_j^*(t)$ position of particle calculated from condition of minimizing game vector along vectors $\boldsymbol{G}$ and $\boldsymbol{G}_C$ of magnetic characteristics uncertainty for games (26) and (27) respectively.

To narrow Pareto set of optimal solutions in (28) – (31) binary preference relations of local games used [49].

**Simulation results.** Let us consider the results of MF modeling of elongated energy-saturated technical object 200 m long and 40 m wide, for which the magnetic silence requirements are set at a control depth of 19 m and 60 m. The initial MF was modeled using 16 dipole sources of the technical object's MF, the measurement of which was performed at 909 points.

For this example, we will consider checking the correctness and efficiency of applying formulas (13) – (15) and (23) – (25). We will check the correctness and efficiency of the formulas on the values of spherical and spheroidal harmonics obtained as a result of optimization. The following harmonic values were obtained:

– for spheroidal $c$ = 45.2171, $c_1^0$ = –2.97466, $c_1^1$ = –0.78397, $s_1^1$ = –1.2093, $c_2^0$ = –7.61832, $c_1^2$ = 1.02365, $c_2^2$ = –0.0247825, $s_2^1$ = 0.321276, $s_2^2$ = 0.0174991, $c_3^0$ = 2.30698, $c_3^1$ = –0.555808, $c_3^2$ = 0.0022228, $c_3^3$ = 0.000110621, $s_3^1$ = 0.856448, $s_3^2$ = –0.0155725, $s_3^3$ = 0.0000373957;

– for spherical $g_1^0$ = –1811.98, $g_1^1$ = 1145.52, $h_1^1$ = 460.332, $g_2^0$ = –2567.85, $g_2^1$ = –13073.2, $g_2^2$ = 3352.89, $h_2^1$ = –16555.6, $h_2^2$ = 6747.55, $g_3^0$ = –54352.8, $g_3^1$ = 38472.4, $g_3^2$ = 22857.2, $g_3^3$ = –9441.96, $h_3^1$ = 18004.4, $h_3^2$ = –31867.1, $h_3^3$ = 8041.49.

These values were obtained on the basis of solving the prediction of the geometric inverse problem of magnetostatics (26) by minimizing the sum of the squares of the differences in the projections of the real MF and the MF models: for spheroidal (13) – (15) and spherical (23) – (25) MF sources up to and including the third harmonics.

The results of calculating the signatures of initial MF (solid lines) with models based on spheroidal (dotted lines) and spherical (dash-dotted lines) harmonics for projections $B_x$ – red, $B_y$ – green, $B_z$ – blue are shown in Fig. 2 – 4, respectively, for 3 cases: $Y$ = –20 m, $Y$ = 0 m and $Y$ = 20 m. Since the technical object is extended, the MF model based on spheroidal harmonics gives better results in approximating the original MF.

The correctness of formulas (23) – (25) for spherical harmonics verified by comparing them with the results obtained by taking numerical partial derivatives with respect to the coordinates $x$, $y$, $z$ from (17) taking into account (18) and standard approach [35]. The calculation results of the proposed method and the standard approach [35] are in full agreement with machine accuracy and differ from the results of numerical differentiation by about $10^{-20}$ $T$.

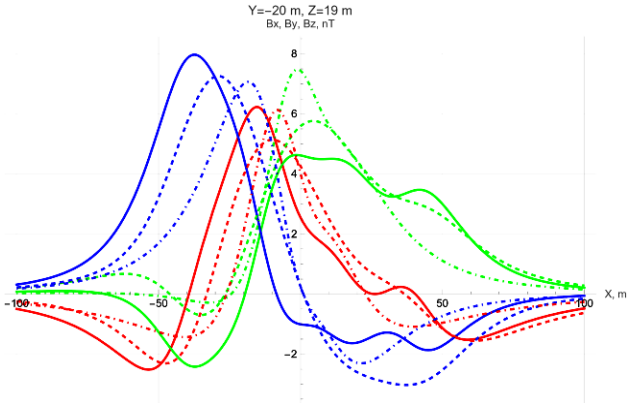


Fig. 2. Magnetic signatures of original, model spherical and model spheroidal MFs for $Y$ = –20 m

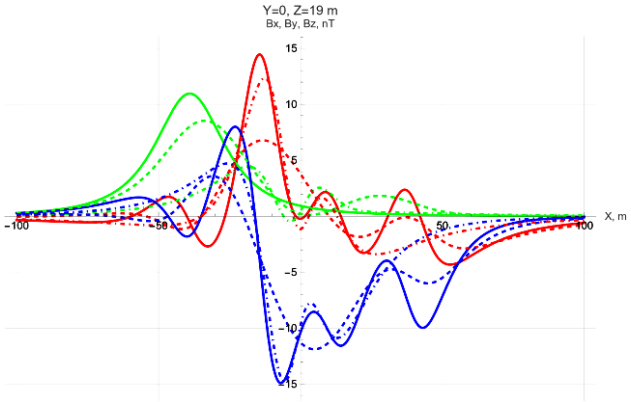


Fig. 3. Magnetic signatures of original, model spherical and model spheroidal magnetic fields for $Y$ = 0 m

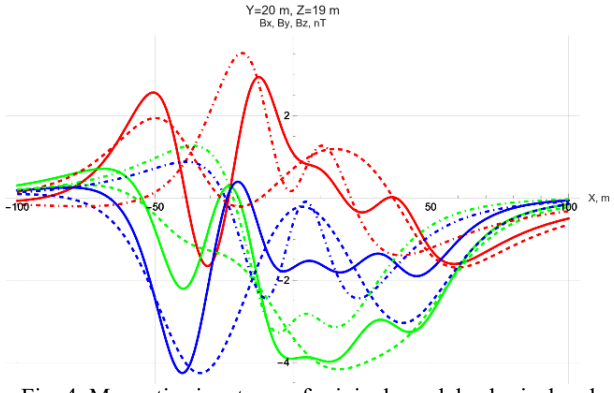


Fig. 4. Magnetic signatures of original, model spherical and model spheroidal MFs for $Y = 20$ m

Table 1 presents a comparison of the calculation time of the standard approach [35] (left column), the proposed method (right column) and the numerical one for spherical harmonics, as well as analytical formulas (13) – (15) taking into account (5) – (8) of the proposed method and the numerical one (numerical taking of derivatives with respect to the coordinates $x$, $y$, $z$ from (4) taking into account (5)) for spheroidal harmonics. The cases of the 1st, 2nd and 3rd harmonics are considered. We see the relative parity in the calculation speed of the proposed method and the standard approach [35] and an order of magnitude faster than the calculation speed of the numerical taking of derivatives in the case of spherical harmonics.

Table 1

Comparison of calculation time of analytical and numerical formulas at $z = 19$ m

| Coordinates and order of harmonics | | | Spherical harmonics | | | | | | Spheroidal harmonics | | | | |
|---|---|---|---|---|---|---|---|---|---|---|---|---|---|
| | | | Projections $\boldsymbol{B}$, nT | | | Time, ms | | | Projections $\boldsymbol{B}$, nT | | | Time, ms | |
| $x$, m | $y$, m | $n$ | $B_x$ | $B_y$ | $B_z$ | Analit. | | Num. | $B_x$ | $B_y$ | $B_z$ | Analit. | Num. |
| –100 | –20 | 1 | –0,326 | 0,005 | 0,134 | 0,229 | 0,296 | 2,622 | –0,351 | –0,016 | 0,313 | 1,492 | 6,486 |
| –100 | –20 | 2 | –0,310 | 0,039 | 0,181 | 0,278 | 0,479 | 7,458 | –0,186 | 0,199 | 0,253 | 3,449 | 18,280 |
| –100 | –20 | 3 | –0,310 | 0,038 | 0,182 | 0,431 | 0,773 | 15,836 | –0,242 | 0,209 | 0,224 | 6,055 | 36,577 |
| –100 | 0 | 1 | –0,302 | 0,109 | 0,134 | 0,189 | 0,293 | 2,543 | –0,326 | 0,130 | 0,328 | 1,474 | 6,601 |
| –100 | 0 | 2 | –0,261 | 0,137 | 0,172 | 0,374 | 0,511 | 7,416 | 0,009 | 0,264 | 0,213 | 3,396 | 18,238 |
| –100 | 0 | 3 | –0,262 | 0,138 | 0,172 | 0,437 | 0,767 | 15,993 | –0,030 | 0,297 | 0,160 | 5,991 | 36,670 |
| –100 | 20 | 1 | –0,211 | 0,177 | 0,112 | 0,195 | 0,293 | 2,628 | –0,199 | 0,218 | 0,278 | 1,501 | 6,505 |
| –100 | 20 | 2 | –0,160 | 0,186 | 0,136 | 0,275 | 0,481 | 7,432 | 0,156 | 0,180 | 0,154 | 3,406 | 17,987 |
| –100 | 20 | 3 | –0,160 | 0,188 | 0,135 | 0,424 | 0,761 | 15,704 | 0,150 | 0,204 | 0,095 | 5,933 | 36,646 |
| –50 | –20 | 1 | –1,615 | –0,420 | 1,231 | 0,187 | 0,291 | 2,574 | –0,535 | –0,430 | 2,786 | 1,472 | 6,474 |
| –50 | –20 | 2 | –1,325 | –0,006 | 1,691 | 0,274 | 0,591 | 7,343 | –1,520 | 1,508 | 2,431 | 3,400 | 18,052 |
| –50 | –20 | 3 | –1,263 | –0,063 | 1,694 | 0,423 | 0,764 | 15,959 | –2,262 | 0,312 | 3,211 | 6,036 | 36,525 |
| –50 | 0 | 1 | –1,620 | 0,749 | 1,366 | 0,187 | 0,290 | 2,543 | 0,785 | 1,574 | 3,295 | 1,478 | 6,607 |
| –50 | 0 | 2 | –0,761 | 1,021 | 1,579 | 0,281 | 0,482 | 7,247 | 2,711 | 4,218 | –2,443 | 3,503 | 17,991 |
| –50 | 0 | 3 | –0,810 | 1,005 | 1,576 | 0,419 | 0,758 | 15,654 | –0,417 | 4,852 | –0,338 | 5,948 | 36,437 |
| –50 | 20 | 1 | –0,483 | 1,198 | 0,800 | 0,201 | 0,291 | 2,565 | 1,286 | 0,864 | 1,385 | 1,487 | 6,476 |
| –50 | 20 | 2 | 0,151 | 0,935 | 0,766 | 0,278 | 0,482 | 7,445 | 2,712 | –1,321 | –1,984 | 3,399 | 18,045 |
| –50 | 20 | 3 | 0,142 | 0,973 | 0,723 | 0,419 | 0,758 | 15,651 | 1,944 | –0,406 | –2,416 | 6,089 | 36,514 |
| 0 | –20 | 1 | 8,631 | 0,137 | 7,246 | 0,188 | 0,289 | 1,812 | 2,736 | 5,201 | 3,174 | 1,948 | 5,292 |
| 0 | –20 | 2 | 7,634 | 9,690 | 3,450 | 0,275 | 0,469 | 3,868 | 4,941 | 1,274 | 3,902 | 4,691 | 13,401 |
| 0 | –20 | 3 | 4,026 | 7,440 | 0,257 | 0,415 | 0,741 | 7,375 | 4,268 | 5,591 | 0,260 | 8,411 | 24,772 |
| 0 | 0 | 1 | 26,417 | 16,701 | –13,423 | 0,194 | 0,295 | 1,802 | 4,472 | 7,874 | –15,782 | 1,777 | 5,036 |
| 0 | 0 | 2 | –11,694 | –14,365 | –33,622 | 0,291 | 0,491 | 3,920 | 1,621 | 2,420 | 4,089 | 4,205 | 12,287 |
| 0 | 0 | 3 | –1,140 | 0,464 | –9,774 | 0,418 | 0,744 | 7,281 | 3,802 | 0,238 | –11,265 | 7,625 | 22,729 |
| 0 | 20 | 1 | 8,631 | –6,433 | –9,102 | 0,190 | 0,289 | 1,812 | 2,736 | –7,051 | –4,769 | 1,945 | 5,323 |
| 0 | 20 | 2 | –2,185 | –0,307 | 1,008 | 0,277 | 0,477 | 3,859 | –1,343 | –0,271 | –1,557 | 4,677 | 13,295 |
| 0 | 20 | 3 | 0,182 | –3,008 | –0,631 | 0,407 | 0,733 | 7,427 | 0,709 | –3,390 | –0,283 | 8,393 | 24,713 |
| 50 | –20 | 1 | –0,915 | 1,370 | –0,470 | 0,192 | 0,291 | 2,591 | –1,382 | 3,024 | –0,495 | 1,481 | 6,491 |
| 50 | –20 | 2 | –1,056 | 1,058 | –0,751 | 0,340 | 0,480 | 7,332 | –2,383 | 4,331 | –3,915 | 3,384 | 18,292 |
| 50 | –20 | 3 | –0,957 | 1,112 | –0,732 | 0,416 | 0,754 | 15,656 | –1,149 | 2,594 | –2,529 | 6,085 | 36,629 |
| 50 | 0 | 1 | –2,220 | 0,749 | –0,993 | 0,183 | 0,287 | 2,528 | –5,443 | 1,574 | –4,364 | 1,493 | 6,578 |
| 50 | 0 | 2 | –1,626 | 0,125 | –1,198 | 0,280 | 0,482 | 7,239 | –4,774 | –1,676 | –8,815 | 3,500 | 18,111 |
| 50 | 0 | 3 | –1,722 | 0,254 | –1,208 | 0,425 | 0,765 | 15,694 | –2,190 | 0,440 | –5,484 | 6,007 | 36,845 |
| 50 | 20 | 1 | –2,047 | –0,593 | –0,900 | 0,200 | 0,293 | 2,617 | –3,203 | –2,591 | –1,896 | 1,483 | 6,513 |
| 50 | 20 | 2 | –1,068 | –0,629 | –0,924 | 0,281 | 0,483 | 7,548 | –0,953 | –3,479 | –2,190 | 3,421 | 18,310 |
| 50 | 20 | 3 | –1,218 | –0,677 | –0,907 | 0,496 | 0,806 | 15,889 | –1,378 | –2,702 | –2,557 | 6,119 | 36,763 |
| 100 | –20 | 1 | –0,255 | 0,186 | –0,038 | 0,193 | 0,290 | 2,561 | –0,422 | 0,273 | 0,039 | 1,479 | 6,688 |
| 100 | –20 | 2 | –0,261 | 0,153 | –0,072 | 0,290 | 0,495 | 7,318 | –0,726 | 0,287 | –0,138 | 3,510 | 18,209 |
| 100 | –20 | 3 | –0,260 | 0,157 | –0,072 | 0,433 | 0,765 | 17,801 | –0,628 | 0,283 | –0,153 | 6,013 | 37,144 |
| 100 | 0 | 1 | –0,350 | 0,109 | –0,055 | 0,187 | 0,288 | 2,552 | –0,584 | 0,130 | 0,011 | 1,470 | 6,455 |
| 100 | 0 | 2 | –0,325 | 0,066 | –0,092 | 0,274 | 0,494 | 7,296 | –0,846 | –0,013 | –0,170 | 3,377 | 18,165 |
| 100 | 0 | 3 | –0,328 | 0,069 | –0,092 | 0,426 | 0,764 | 15,637 | –0,764 | 0,032 | –0,194 | 6,155 | 36,744 |
| 100 | 20 | 1 | –0,369 | –0,004 | –0,060 | 0,191 | 0,293 | 2,570 | –0,574 | –0,071 | 0,004 | 1,470 | 6,600 |
| 100 | 20 | 2 | –0,316 | –0,034 | –0,093 | 0,286 | 0,489 | 7,321 | –0,672 | –0,273 | –0,122 | 3,507 | 18,187 |
| 100 | 20 | 3 | –0,321 | –0,033 | –0,091 | 0,427 | 0,764 | 15,924 | –0,650 | –0,222 | –0,151 | 6,076 | 37,415 |

In the case of spheroidal harmonics, the difference in the calculation speed between the analytical and numerical methods is not as pronounced as for spherical ones, but it still takes place – by 4 or more times. Moreover, in all cases, with an increase in the order of the harmonic, this difference only increases. Let us now proceed to checking the correctness of formulas (13) – (15). The results of comparing the calculation using these formulas with the results calculated by taking numerical partial derivatives with respect to the coordinates $x$, $y$, $z$ from (4) taking into account (5) are also consistent and differ by a deviation of about $10^{-20}$ $T$. Another way of checking is to consider the MF of a dipole and a spheroid (the case of the 1st harmonic) with an equivalent magnetic moment at large distances from the source.

It is necessary to equate the 1st spheroidal harmonics in this way [13]:

$$c_1^0 = \frac{3}{c^2} g_1^0, \quad c_1^1 = \frac{3}{2c^2} g_1^1, \quad s_1^1 = -\frac{3}{2c^2} h_1^1.$$

And for dipole model [50, formulas (2), (3)]:

$$M_x = g_1^0, \quad M_y = -g_1^1, \quad M_z = -h_1^1.$$

Let us consider the points located on the rays from the source in all 8 coordinate octants. The rays pass through points $N_P$. The distance from the center on these rays is $R_P$.

Table 2 presents the results of comparing the projections of the MF of the spheroidal model and the dipole model with an equivalent magnetic moment. As the distance from the field source increases, the relative discrepancies tend to zero.

Table 2

Asymptotic verification of the correctness of formulas (13) – (15) for the case of the 1st harmonic

| Direction vector and distance | | Projections $\boldsymbol{B}$, nT | | | | | | Relative divergence, % | | |
|---|---|---|---|---|---|---|---|---|---|---|
| | | Spheroidal harmonics | | | Dipole model | | | | | |
| $N_P$ | $R_P$ | $B_x$ | $B_y$ | $B_z$ | $B_x$ | $B_y$ | $B_z$ | $\Delta_x$ | $\Delta_y$ | $\Delta_z$ |
| {–1;–1;–1} | 1 | 16,0 | –771,6 | –1903,5 | –30904,7 | –43730,6 | –56917,1 | 100,1 | 98,2 | 96,7 |
| {–1;–1;–1} | 10 | 2,8 | –11,1 | –20,4 | –30,9 | –43,7 | –56,9 | 109,2 | 74,7 | 64,2 |
| {–1;–1;–1} | 100 | –0,02801 | –0,04392 | –0,05727 | –0,03090 | –0,04373 | –0,05692 | 9,352 | 0,423 | 0,618 |
| {–1;–1;–1} | 1000 | –0,00003 | –0,00004 | –0,00006 | –0,00003 | –0,00004 | –0,00006 | 0,094 | 0,007 | 0,009 |
| {–1;–1;1} | 1 | 17,5 | 754,0 | 1898,8 | –13186,5 | –26012,4 | 56917,1 | 100,1 | 102,9 | 96,7 |
| {–1;–1;1} | 10 | 4,1 | 2,8 | 19,1 | –13,2 | –26,0 | 56,9 | 131,3 | 110,7 | 66,4 |
| {–1;–1;1} | 100 | –0,01074 | –0,02543 | 0,05673 | –0,01319 | –0,02601 | 0,05692 | 18,576 | 2,222 | 0,329 |
| {–1;–1;1} | 1000 | –0,00001 | –0,00003 | 0,00006 | –0,00001 | –0,00003 | 0,00006 | 0,191 | 0,019 | 0,001 |
| {–1;1;–1} | 1 | 19,7 | 759,9 | 1892,9 | 13186,5 | 43730,6 | –12825,9 | 99,9 | 98,3 | 114,8 |
| {–1;1;–1} | 10 | 6,0 | 7,8 | 14,0 | 13,2 | 43,7 | –12,8 | 54,2 | 82,1 | 209,5 |
| {–1;1;–1} | 100 | 0,01498 | 0,04257 | –0,01128 | 0,01319 | 0,04373 | –0,01283 | 13,603 | 2,644 | 12,062 |
| {–1;1;–1} | 1000 | 0,00001 | 0,00004 | –0,00001 | 0,00001 | 0,00004 | –0,00001 | 0,145 | 0,025 | 0,118 |
| {–1;1;1} | 1 | 21,2 | –765,7 | –1897,6 | 30904,7 | 26012,4 | 12825,9 | 99,9 | 102,9 | 114,8 |
| {–1;1;1} | 10 | 7,3 | –6,0 | –15,3 | 30,9 | 26,0 | 12,8 | 76,3 | 123,1 | 219,6 |
| {–1;1;1} | 100 | 0,03226 | 0,02409 | 0,01074 | 0,03090 | 0,02601 | 0,01283 | 4,378 | 7,379 | 16,265 |
| {–1;1;1} | 1000 | 0,00003 | 0,00003 | 0,00001 | 0,00003 | 0,00003 | 0,00001 | 0,049 | 0,073 | 0,162 |
| {1;–1;–1} | 1 | 21,2 | –765,7 | –1897,6 | 30904,7 | 26012,4 | 12825,9 | 99,9 | 102,9 | 114,8 |
| {1;–1;–1} | 10 | 7,3 | –6,0 | –15,3 | 30,9 | 26,0 | 12,8 | 76,3 | 123,1 | 219,6 |
| {1;–1;–1} | 100 | 0,03226 | 0,02409 | 0,01074 | 0,03090 | 0,02601 | 0,01283 | 4,378 | 7,379 | 16,265 |
| {1;–1;–1} | 1000 | 0,00003 | 0,00003 | 0,00001 | 0,00003 | 0,00003 | 0,00001 | 0,049 | 0,073 | 0,162 |
| {1;–1;1} | 1 | 19,7 | 759,9 | 1892,9 | 13186,5 | 43730,6 | –12825,9 | 99,9 | 98,3 | 114,8 |
| {1;–1;1} | 10 | 6,0 | 7,8 | 14,0 | 13,2 | 43,7 | –12,8 | 54,2 | 82,1 | 209,5 |
| {1;–1;1} | 100 | 0,01498 | 0,04257 | –0,01128 | 0,01319 | 0,04373 | –0,01283 | 13,603 | 2,644 | 12,062 |
| {1;–1;1} | 1000 | 0,00001 | 0,00004 | –0,00001 | 0,00001 | 0,00004 | –0,00001 | 0,145 | 0,025 | 0,118 |
| {1;1;–1} | 1 | 17,5 | 754,0 | 1898,8 | –13186,5 | –26012,4 | 56917,1 | 100,1 | 102,9 | 96,7 |
| {1;1;–1} | 10 | 4,1 | 2,8 | 19,1 | –13,2 | –26,0 | 56,9 | 131,3 | 110,7 | 66,4 |
| {1;1;–1} | 100 | –0,01074 | –0,02543 | 0,05673 | –0,01319 | –0,02601 | 0,05692 | 18,576 | 2,222 | 0,329 |
| {1;1;–1} | 1000 | –0,00001 | –0,00003 | 0,00006 | –0,00001 | –0,00003 | 0,00006 | 0,191 | 0,019 | 0,001 |
| {1;1;1} | 1 | 16,0 | –771,6 | –1903,5 | –30904,7 | –43730,6 | –56917,1 | 100,1 | 98,2 | 96,7 |
| {1;1;1} | 10 | 2,8 | –11,1 | –20,4 | –30,9 | –43,7 | –56,9 | 109,2 | 74,7 | 64,2 |
| {1;1;1} | 100 | –0,02801 | –0,04392 | –0,05727 | –0,03090 | –0,04373 | –0,05692 | 9,352 | 0,423 | 0,618 |
| {1;1;1} | 1000 | –0,00003 | –0,00004 | –0,00006 | –0,00003 | –0,00004 | –0,00006 | 0,094 | 0,007 | 0,009 |

**Conclusions.**

1. For the first time a simplified method of mathematical modeling of the external magnetic field of an uncertain extended technical object is proposed, based on the analytical calculation of the magnetic field induction of spherical and spheroidal sources in the Cartesian coordinate system. Unlike known methods, this method allows modeling the magnetic field directly in the Cartesian coordinate system without finding the projection of the magnetic induction in the prolate spheroidal coordinate system and the spherical coordinate system and without their translation from the prolate spheroidal coordinate system and the spherical coordinate system to the Cartesian coordinate system and vice versa.

2. Promising magnetostatics problems are solved using the proposed method based on near-field measurements. Geometric inverse magnetostatics problems for predicting and controlling the magnetic silence of a technical object are calculated based on solving vector games. The payoff in both vector games is calculated as a solution to direct problems using the Wolfram Mathematica software package.

3. The use of the proposed simplified method allows to reduce the calculation time for determining the magnetic field induction of elongated spheroidal magnetic field sources by more than 10 times and makes it possible to reduce the calculation time of magnetic field induction of spherical magnetic field sources by more than 4 times.

4. In the future, it is planned to conduct experimental studies of the efficiency of modeling and reducing the magnetic field of uncertain extended technical objects based on the developed method.

**Conflict of interest.** The authors declare that they have no conflicts of interest.

REFERENCES


***1.*** Rozov V.Yu., Getman A.V., Petrov S.V., Erisov A.V., Melanchenko A.G., Khoroshilov V.S., Schmidt I.R Spacecraft magnetism. *Technical Electrodynamics. Thematic issue «Problems of modern electrical engineering»*, 2010, part 2, pp. 144-147. (Rus).

***2.*** *ECSS-E-HB-20-07A. Space engineering: Electromagnetic compatibility hand-book. ESA-ESTEC. Requirements & Standards Division*. Noordwijk, Netherlands, 2012. 228 p.

***3.*** Droughts S.A., Fedorov O.P. Space project Ionosat-Micro. Monograph. Kyiv, Akademperiodika Publ., 2013. 218 p. (Rus).

***4.*** Holmes J.J. *Exploitation of A Ship's Magnetic Field Signatures*. Springer Cham, 2006. 67 p. doi: https://doi.org/10.1007/978-3-031-01693-6.

***5.*** Woloszyn M., Jankowski P. Simulation of ship's deperming process using Opera 3D. 2017 18th International Symposium on Electromagnetic Fields in Mechatronics, Electrical and Electronic Engineering (ISEF) Book of Abstracts, 2017, pp. 1-2. doi: https://doi.org/10.1109/ISEF.2017.8090680.

***6.*** Birsan M., Holtham P., Carmen. Using global optimisation techniques to solve the inverse problem for the computation of the static magnetic signature of ships. *Defense Research Establishment Atlantic*, 9 Grove St., PO Box 1012, Dartmouth, Nova Scotia, B2Y 3Z7, Canada.

***7.*** Zuo C., Ma M., Pan Y., Li M., Yan H., Wang J., Geng P., Ouyang J. Multi-objective optimization design method of naval vessels degaussing coils. *Proceedings of SPIE - The International Society for Optical Engineering*, 2022, vol. 12506, art. no. 125060J. doi: https://doi.org/10.1117/12.2662888.

***8.*** Baranov M.I., Rozov V.Y., Sokol Y.I. To the 100th anniversary of the National Academy of Sciences of Ukraine – the cradle of domestic science and technology. *Electrical Engineering & Electromechanics*, 2018, no. 5, pp. 3-11. doi: https://doi.org/10.20998/2074-272X.2018.5.01.

***9.*** Chadebec O., Rouve L.-L., Coulomb J.-L. New methods for a fast and easy computation of stray fields created by wound rods. *IEEE Transactions on Magnetics*, 2002, vol. 38, no. 2, pp. 517-520. doi: https://doi.org/10.1109/20.996136.

***10.*** Rozov V.Yu. Methods for reducing external magnetic fields of energy-saturated objects. *Technical Electrodynamics*, 2001, no. 1, pp. 16-20.

***11.*** Rozov V.Y., Tkachenko O.O., Yerisov A.V., Grinchenko V.S. Analytical calculation of magnetic field of three-phase cable lines with two-point bonded shields. *Technical Electrodynamics*, 2017, no. 2, pp. 13-18. (Rus). doi: https://doi.org/10.15407/techned2017.02.013.

***12.*** Rozov V.Y., Pelevin D.Y., Kundius K.D. Simulation of the magnetic field in residential buildings with built-in substations based on a two-phase multi-dipole model of a three-phase current conductor. *Electrical Engineering & Electromechanics*, 2023, no. 5, pp. 87-93. doi: https://doi.org/10.20998/2074-272X.2023.5.13.

***13.*** Rozov V.Yu., Getman A.V., Kildishev A.V. Spatial harmonic analysis of the external magnetic field of extended objects in a prolate spheroidal coordinate system. *Technical Electrodynamics*, 1999, no. 1, pp. 7-11. (Rus).

***14.*** Rozov V.Yu. Mathematical model of electrical equipment as a source of external magnetic field. *Technical Electrodynamics*, 1995, no. 2, pp. 3-7. (Rus).

***15.*** Volokhov S.A., Dobrodeev P.N., Ivleva L.F. Spatial harmonic analysis of the external magnetic field of a technical object. *Technical Electrodynamics*, 1996, no. 2, pp. 3-8. (Rus).

***16.*** Getman A.V. *Analysis and synthesis of the magnetic field structure of technical objects on the basis of spatial harmonics*. Dissertation thesis for the degree of Doctor of Technical Sciences. Kharkiv, 2018. 43 p. (Ukr).

***17.*** Xiao C., Xiao C., Li G. Modeling the ship degaussing coil's effect based on magnetization method. *Communications in Computer and Information Science*, 2012, vol. 289, pp. 62-69. doi: https://doi.org/10.1007/978-3-642-31968-6_8.

***18.*** Wołoszyn M., Jankowski P. Ship's de-perming process using coils lying on seabed. *Metrology and Measurement Systems*, 2019, vol. 26, no. 3, pp. 569-579. doi: https://doi.org/10.24425/mms.2019.129582.

***19.*** Fan J., Zhao W., Liu S., Zhu Z. Summary of ship comprehensive degaussing. *Journal of Physics: Conference Series*, 2021, vol. 1827, no. 1, art. no. 012014. doi: https://doi.org/10.1088/1742-6596/1827/1/012014.

***20.*** Getman A.V. Spatial harmonic analysis of the magnetic field of the sensor of the neutral plasma component. *Eastern European Journal of Advanced Technologies*, 2010, vol. 6, no. 5(48), pp. 35-38. doi: https://doi.org/10.15587/1729-4061.2010.3326.

***21.*** Getman A. Ensuring the Magnetic Compatibility of Electronic Components of Small Spacecraft. *2022 IEEE 3rd KhPI Week on Advanced Technology (KhPIWeek)*, 2022, no. 1-4. doi: https://doi.org/10.1109/KhPIWeek57572.2022.9916339.

***22.*** Acuña M.H. *The design, construction and test of magnetically clean spacecraft – a practical guide*. NASA/GSFC internal report. 2004.

***23.*** Junge A., Marliani F. Prediction of DC magnetic fields for magnetic cleanliness on spacecraft. *2011 IEEE International Symposium on Electromagnetic Compatibility*, 2011, pp. 834-839. doi: https://doi.org/10.1109/ISEMC.2011.6038424.

***24.*** Lynn G.E., Hurt J.G., Harriger K.A. Magnetic control of satellite attitude. *IEEE Transactions on Communication and Electronics*, 1964, vol. 83, no. 74, pp. 570-575. doi: https://doi.org/10.1109/TCOME.1964.6539511.

***25.*** Junge A., Trougnou L., Carrubba E. Measurement of Induced Equivalent Magnetic Dipole Moments for Spacecraft Units and Components. *Proceedings ESA Workshop Aerospace EMC 2009 ESA WPP-299*, 2009, vol. 4, no. 2, pp. 131-140.

***26.*** Mehlem K., Wiegand A. Magnetostatic cleanliness of spacecraft. *2010 Asia-Pacific International Symposium on Electromagnetic Compatibility*, 2010, pp. 936-944. doi: https://doi.org/10.1109/APEMC.2010.5475692.

***27.*** Messidoro P., Braghin M., Grande M. Magnetic cleanliness verification approach on tethered satellite. *16th Space Simulation Conference: Confirming Spaceworthiness into the Next Millennium*, 1991, pp. 415-434.

***28.*** Mehlem K., Narvaez P. Magnetostatic cleanliness of the radioisotope thermoelectric generators (RTGs) of Cassini. *1999 IEEE International Symposium on Electromagnetic Compatability*, 1999, vol. 2, pp. 899-904. doi: https://doi.org/10.1109/ISEMC.1999.810175.

***29.*** Eichhorn W.L. *Magnetic dipole moment determination by near-field analysis*. Goddard Space Flight Center. Washington, D.C., National Aeronautics and Space Administration, 1972. NASA technical note, D 6685. 87 p.

***30.*** Matsushima M., Tsunakawa H., Iijima Y., Nakazawa S., Matsuoka A., Ikegami S., Ishikawa T., Shibuya H., Shimizu H., Takahashi F. Magnetic Cleanliness Program Under Control of Electromagnetic Compatibility for the SELENE (Kaguya) Spacecraft. *Space Science Reviews*, 2010, vol. 154, no. 1-4, pp. 253-264. doi: https://doi.org/10.1007/s11214-010-9655-x.

***31.*** Boghosian M., Narvaez P., Herman R. Magnetic testing, and modeling, simulation and analysis for space applications. *2013 IEEE International Symposium on Electromagnetic Compatibility*, 2013, pp. 265-270. doi: https://doi.org/10.1109/ISEMC.2013.6670421.

***32.*** Mehlem K. Multiple magnetic dipole modeling and field prediction of satellites. *IEEE Transactions on Magnetics*, 1978, vol. 14, no. 5, pp. 1064-1071. doi: https://doi.org/10.1109/TMAG.1978.1059983.

***33.*** Thomsen P.L., Hansen F. Danish Ørsted Mission In-Orbit Experiences and Status of The Danish Small Satellite Programme. *Annual AIAA/USU Conference on Small Satellites*, 1999, pp. SSC99-I–8.

***34.*** Kapsalis N.C., Kakarakis S.-D.J., Capsalis C.N. Prediction of multiple magnetic dipole model parameters from near field measurements employing stochastic algorithms. *Progress In Electromagnetics Research Letters*, 2012, vol. 34, pp. 111-122. doi: https://doi.org/10.2528/PIERL12030905.

**35.** Rozov V.Yu., Dobrodeev P.N., Volokhov S.A. Multipole model of a technical object and its magnetic center. *Technical Electrodynamics*, 2008, no. 2, pp. 3-8. (Rus).
**36.** Abramowitz M., Stegun I.A. (ed.). *Handbook of mathematical functions with formulas, graphs, and mathematical tables*. US Government Printing Office Publ., 1964. 1046 p.
**37.** Solomentsev O., Zaliskyi M., Averyanova Y., Ostroumov I., Kuzmenko N., Sushchenko O., Kuznetsov B., Nikitina T., Tserne E., Pavlikov V., Zhyla S., Dergachov K., Havrylenko O., Popov A., Volosyuk V., Ruzhentsev N., Shmatko O. Method of Optimal Threshold Calculation in Case of Radio Equipment Maintenance. *Data Science and Security. Lecture Notes in Networks and Systems*, 2022, vol. 462, pp. 69-79. doi: https://doi.org/10.1007/978-981-19-2211-4_6.
**38.** Ruzhentsev N., Zhyla S., Pavlikov V., Volosyuk V., Tserne E., Popov A., Shmatko O., Ostroumov I., Kuzmenko N., Dergachov K., Sushchenko O., Averyanova Y., Zaliskyi M., Solomentsev O., Havrylenko O., Kuznetsov B., Nikitina T. Radio-Heat Contrasts of UAVs and Their Weather Variability at 12 GHz, 20 GHz, 34 GHz, and 94 GHz Frequencies. *ECTI Transactions on Electrical Engineering, Electronics, and Communications*, 2022, vol. 20, no. 2, pp. 163-173. doi: https://doi.org/10.37936/ecti-eec.2022202.246878.
**39.** Havrylenko O., Dergachov K., Pavlikov V., Zhyla S., Shmatko O., Ruzhentsev N., Popov A., Volosyuk V., Tserne E., Zaliskyi M., Solomentsev O., Ostroumov I., Sushchenko O., Averyanova Y., Kuzmenko N., Nikitina T., Kuznetsov B. Decision Support System Based on the ELECTRE Method. *Data Science and Security. Lecture Notes in Networks and Systems*, 2022, vol. 462, pp. 295-304. doi: https://doi.org/10.1007/978-981-19-2211-4_26.
**40.** Shmatko O., Volosyuk V., Zhyla S., Pavlikov V., Ruzhentsev N., Tserne E., Popov A., Ostroumov I., Kuzmenko N., Dergachov K., Sushchenko O., Averyanova Y., Zaliskyi M., Solomentsev O., Havrylenko O., Kuznetsov B., Nikitina T. Synthesis of the optimal algorithm and structure of contactless optical device for estimating the parameters of statistically uneven surfaces. *Radioelectronic and Computer Systems*, 2021, no. 4, pp. 199-213. doi: https://doi.org/10.32620/reks.2021.4.16.
**41.** Volosyuk V., Zhyla S., Pavlikov V., Ruzhentsev N., Tserne E., Popov A., Shmatko O., Dergachov K., Havrylenko O., Ostroumov I., Kuzmenko N., Sushchenko O., Averyanova Yu., Zaliskyi M., Solomentsev O., Kuznetsov B., Nikitina T. Optimal Method for Polarization Selection of Stationary Objects Against the Background of the Earth's Surface. *International Journal of Electronics and Telecommunications*, 2022, vol. 68, no. 1, pp. 83-89. doi: https://doi.org/10.24425/ijet.2022.139852.
**42.** Zhyla S., Volosyuk V., Pavlikov V., Ruzhentsev N., Tserne E., Popov A., Shmatko O., Havrylenko O., Kuzmenko N., Dergachov K., Averyanova Y., Sushchenko O., Zaliskyi M., Solomentsev O., Ostroumov I., Kuznetsov B., Nikitina T. Practical imaging algorithms in ultra-wideband radar systems using active aperture synthesis and stochastic probing signals. *Radioelectronic and Computer Systems*, 2023, no. 1, pp. 55-76. doi: https://doi.org/10.32620/reks.2023.1.05.
**43.** Maksymenko-Sheiko K.V., Sheiko T.I., Lisin D.O., Petrenko N.D. Mathematical and Computer Modeling of the Forms of Multi-Zone Fuel Elements with Plates. *Journal of Mechanical Engineering*, 2022, vol. 25, no. 4, pp. 32-38. doi: https://doi.org/10.15407/pmach2022.04.032.
**44.** Hontarovskyi P.P., Smetankina N.V., Ugrimov S.V., Garmash N.H., Melezhyk I.I. Computational Studies of the Thermal Stress State of Multilayer Glazing with Electric Heating. *Journal of Mechanical Engineering*, 2022, vol. 25, no. 1, pp. 14-21. doi: https://doi.org/10.15407/pmach2022.02.014.
**45.** Kostikov A.O., Zevin L.I., Krol H.H., Vorontsova A.L. The Optimal Correcting the Power Value of a Nuclear Power Plant Power Unit Reactor in the Event of Equipment Failures. *Journal of Mechanical Engineering*, 2022, vol. 25, no. 3, pp. 40-45. doi: https://doi.org/10.15407/pmach2022.03.040.
**46.** Rusanov A.V., Subotin V.H., Khoryev O.M., Bykov Y.A., Korotaiev P.O., Ahibalov Y.S. Effect of 3D Shape of Pump-Turbine Runner Blade on Flow Characteristics in Turbine Mode. *Journal of Mechanical Engineering*, 2022, vol. 25, no. 4, pp. 6-14. doi: https://doi.org/10.15407/pmach2022.04.006.
**47.** Gontarovskyi P., Smetankina N., Garmash N., Melezhyk I. Numerical analysis of stress-strain state of fuel tanks of launch vehicles in 3D formulation. *Lecture Notes in Networks and Systems*, 2021, vol. 188, pp. 609–619. doi: https://doi.org/10.1007/978-3-030-66717-7_52.
**48.** Kurennov S., Smetankina N., Pavlikov V., Dvoretskaya D., Radchenko V. Mathematical Model of the Stress State of the Antenna Radome Joint with the Load-Bearing Edging of the Skin Cutout. *Lecture Notes in Networks and Systems*, 2022, vol. 305, pp. 287-295. doi: https://doi.org/10.1007/978-3-030-83368-8_28.
**49.** Sushchenko O., Averyanova Y., Ostroumov I., Kuzmenko N., Zaliskyi M., Solomentsev O., Kuznetsov B., Nikitina T., Havrylenko O., Popov A., Volosyuk V., Shmatko O., Ruzhentsev N., Zhyla S., Pavlikov V., Dergachov K., Tserne E. Algorithms for Design of Robust Stabilization Systems. *Lecture Notes in Computer Science*, 2022, vol. 13375, pp. 198-213. doi: https://doi.org/10.1007/978-3-031-10522-7_15.
**50.** Sheinker A., Ginzburg B., Salomonski N., Yaniv A., Persky E. Estimation of Ship's Magnetic Signature Using Multi-Dipole Modeling Method. *IEEE Transactions on Magnetics*, 2021, vol. 57, no. 5, pp. 1-8. doi: https://doi.org/10.1109/TMAG.2021.3062998.

*Received 06.10.2024*
*Accepted 20.01.2025*
*Published 02.05.2025*

*B.I. Kuznetsov*[1], *Doctor of Technical Science, Professor,*
*T.B. Nikitina*[2], *Doctor of Technical Science, Professor,*
*I.V. Bovdui*[1], *PhD, Senior Research Scientist,*
*K.V. Chunikhin*[1], *PhD, Senior Research Scientist,*
*V.V. Kolomiets*[2], *PhD, Assistant Professor,*
*I.V. Nefodova*[2], *PhD, Assistant Professor*
[1] Anatolii Pidhornyi Institute of Power Machines and Systems of the National Academy of Sciences of Ukraine,
2/10, Komunalnykiv Str., Kharkiv, 61046, Ukraine,
e-mail: kuznetsov.boris.i@gmail.com (Corresponding Author)
[2] Bakhmut Education Research and Professional Pedagogical Institute V.N. Karazin Kharkiv National University,
9a, Nosakov Str., Bakhmut, Donetsk Region, 84511, Ukraine.

*How to cite this article:*
Kuznetsov B.I., Nikitina T.B., Bovdui I.V., Chunikhin K.V., Kolomiets V.V., Nefodova I.V. Simplified method for analytically determining the external magnetostatic field of uncertain extended technical objects based on near-field measurements. *Electrical Engineering & Electromechanics*, 2025, no. 3, pp. 65-75. doi: https://doi.org/10.20998/2074-272X.2025.3.10